Journal of Alloys and Compounds 504S (2010) S106–S109

Contents lists available at ScienceDirect

Journal of Alloys and Compounds

journal homepage: www.elsevier.com/locate/jallcom

$W_f/Zr_{41.2}Ti_{13.8}Cu_{12.5}Ni_{10}Be_{22.5}$ bulk metallic glass composites prepared by a new melt infiltrating method

H.T. Zong[a], M.Z. Ma[a], L. Liu[a,b], X.Y. Zhang[a], B.W. Bai[a], P.F. Yu[a], L. Qi[a], Q. Jing[a,b], G. Li[a,b], R.P. Liu[a,*]

[a] State Key Laboratory of Metastable Materials Science and Technology, Yanshan University, Qinhuangdao 066004, China
[b] College of Electronic and Information Engineering, Hebei University, Baoding 071000, China

ARTICLE INFO

Article history:
Received 26 June 2009
Received in revised form 7 January 2010
Accepted 10 February 2010
Available online 17 February 2010

Keywords:
Bulk metallic glass composite
Inverted melt infiltrating casting
Compressive strength
Capillarity

ABSTRACT

$W_f/Zr_{41.2}Ti_{13.8}Cu_{12.5}Ni_{10}Be_{22.5}$ bulk metallic glass composites were successfully prepared by a new inverted melt infiltrating method. The processing parameters were optimized by adjusting infiltrating temperature, infiltrating time and tungsten fibers' volume fraction. The diameter of the tungsten fiber was found to have remarkable influence on compressive properties and fracture mode of the composites. The $W_f/Zr_{41.2}Ti_{13.8}Cu_{12.5}Ni_{10}Be_{22.5}$ bulk metallic glass composites reinforced with 50% volume fraction tungsten fiber (200 μm in diameter) exhibited the highest compressive strength and plastic strain up to 2146 MPa and 21.4%, respectively. Besides, the shear bands are found to get closer as the diameter of the tungsten fibers decreases.

1. Introduction

Bulk metallic glasses (BMGs) have many potential applications due to their unique properties, such as superior strength and hardness, excellent corrosion resistance and high wear resistance [1–5]. The $Zr_{41.2}Ti_{13.8}Cu_{12.5}Ni_{10}Be_{22.5}$ (Vitreloy 1) BMG exhibits an exceptional glass forming ability with a critical cooling rate of ∼1 K/s as well as shows a tensile strength of 1.9 GPa and an elastic strain limit of 2% under compressive or tensile loading [6–8]. However, Vitreloy 1, like all other metallic glasses, fails to form highly localized shear bands, which leads to catastrophic failure under unconstrained conditions without much macroscopic plasticity [6,7,9]. Fortunately, the development of BMG matrix composites (BMGC) opens new opportunities for the application of metallic glasses. Researchers attempted to introduce a second phase to prevent the brittle fracture of the monolithic BMGs and ductile metallic fibers or, in particular, were used to reinforce BMGs [10–14]. Conner et al. found that tungsten fiber (W_f) reinforced BMGs increased compressive strain to failure by over 900% compared to the unreinforced ones and the fracture surface behaves like a slurry flow [10]. This was ascribed to the local melting in the matrix due to the temperature rise in the shear band, and further this leads to viscous flow [15,16]. In the past few years, the deformation behaviors of W_f/Zr-based BMGC under quasi-static and dynamic compression condition were investigated [3,10,15,17]. $W_f/Zr_{41.2}Ti_{13.8}Cu_{12.5}Ni_{10}Be_{22.5}$ BMGC have been successfully fabricated using pressure infiltration by Johnson's group [2]. In the present work, we developed a new melt infiltrating method, inverted melt infiltrating casting (IMIC), to prepared $W_f/Zr_{41.2}Ti_{13.8}Cu_{12.5}Ni_{10}Be_{22.5}$ BMGC. The effect of the diameter of the tungsten fibers on the compressive behaviors of the $W_f/Zr_{41.2}Ti_{13.8}Cu_{12.5}Ni_{10}Be_{22.5}$ BMGC was studied.

2. Experimental

$Zr_{41.2}Ti_{13.8}Cu_{12.5}Ni_{10}Be_{22.5}$ ingots were prepared by arc-melting elements with a purity ranging from 99.5 to 99.99% in a titanium-gathered argon atmosphere. The alloy melts were then cast into a copper mould to obtain amorphous alloy rods with 5 mm in diameter, 70 mm in length. Tungsten fibers with 200 μm, 500 μm and 750 μm in diameter were first straightened and cut to 50 mm in length, then cleaned in an ultrasonic bath of acetone, followed by ethanol after dipping in hydrofluoric acid for 12 h to remove surface impurity.

We adopted inverted melt infiltrating casting method to prepare the composite samples with 5 mm in diameter and 50 mm in length. A bundle of tungsten fibers tightly arranged in advance was placed on top of a $Zr_{41.2}Ti_{13.8}Cu_{12.5}Ni_{10}Be_{22.5}$ alloy rod in a quartz tube and then encapsulated with high vacuum. Samples were heated in an electrical resistance furnace, when the alloy rod was melted, the tungsten fibers were slowly immersed into the melt by gravitation and the melt infiltrated through the tungsten fibers under capillarity effect synchronously. Finally, when tungsten fibers were entirely immersed into the alloy melt, quartz tubes were quenched in a brine solution. In order to control the interface reaction and obtain a favorable interface, infiltrating temperature and infiltrating time turn out to be two key parameters. The process is optimized at an infiltrating temperature of 1173 K for 30 min. Fig. 1 was the diagrammatic sketch of the inverted melt infiltrating process and $W_f/Zr_{41.2}Ti_{13.8}Cu_{12.5}Ni_{10}Be_{22.5}$ BMGC rods. W fibers in $W_f/Zr_{41.2}Ti_{13.8}Cu_{12.5}Ni_{10}Be_{22.5}$ bulk metallic glass composites prepared by our new infiltrating method distribute homogeneously and keep a good verticality when W fibers volume fraction was above 40%.

* Corresponding author. Tel.: +86 335 8074723; fax: +86 335 8074545.
E-mail address: riping@ysu.edu.cn (R.P. Liu).

0925-8388/$ – see front matter © 2010 Elsevier B.V. All rights reserved.
doi:10.1016/j.jallcom.2010.02.045

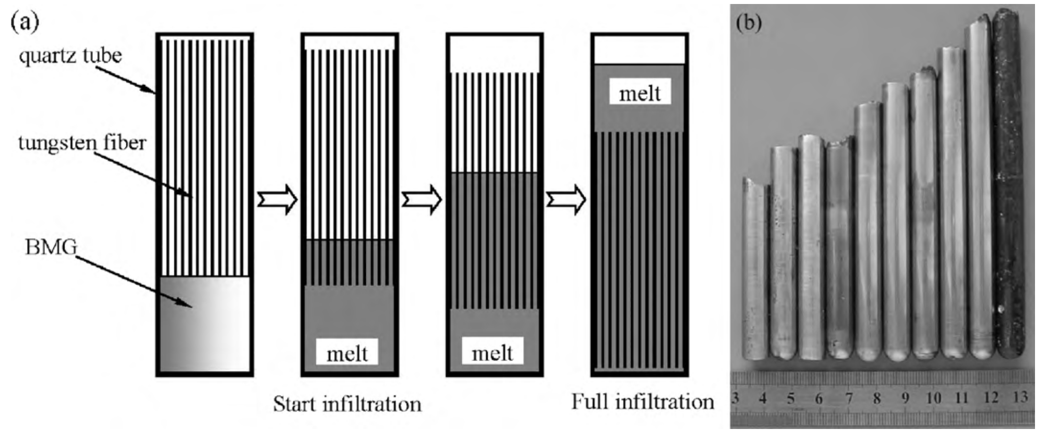

Fig. 1. Diagrammatic sketch of the inverted melt infiltrating process and BMGC rods.

Cylindrical specimens with 5 mm in diameter and an aspect ratio of 3:2 were prepared for compression test and the ends of all the specimens were carefully polished to make them parallel to each other. The ends of the compression samples were lubricated with MoS_2 to prevent "barreling" of the sample. The compression samples were sandwiched between two WC platens in a loading fixture to guarantee axial loading. The uniaxial compression tests were conducted on a WDW-3050 type testing machine at constant strain rate about $6 \times 10^{-4}\, s^{-1}$. The fracture surface was analyzed using KYKY-2800 scanning electron microscope (SEM).

3. Results and discussion

Fig. 2 shows the compressive stress–strain curves of $W_f/Zr_{41.2}Ti_{13.8}Cu_{12.5}Ni_{10}Be_{22.5}$ BMGC reinforced with W_f of 750 µm, 500 µm and 200 µm in diameter. As shown in Fig. 2, when the W_f volume fraction was less than 45%, the $W_f/Zr_{41.2}Ti_{13.8}Cu_{12.5}Ni_{10}Be_{22.5}$ BMGC exhibited little or no plastic strain, while when the W_f volume fraction was increased to

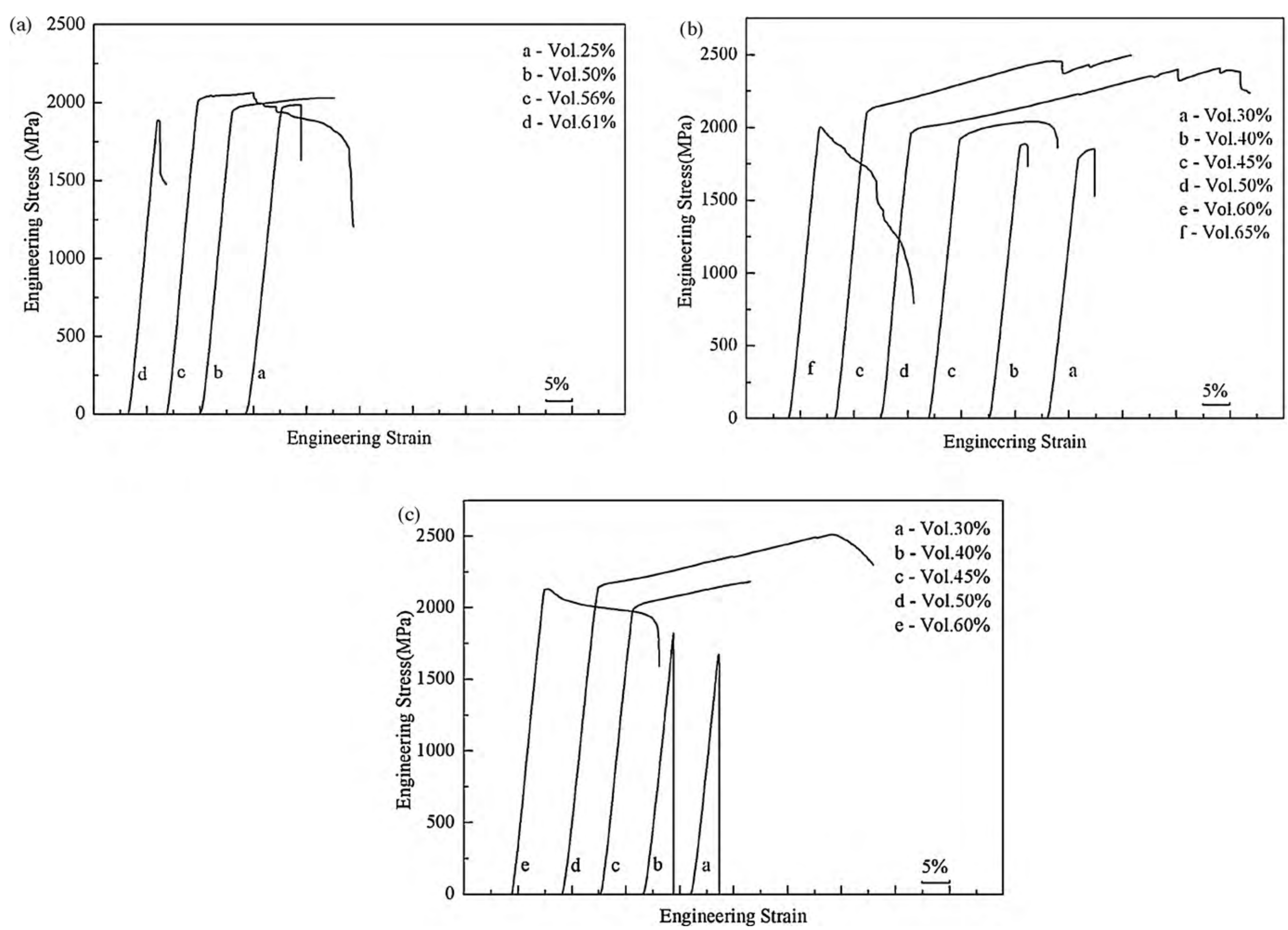

Fig. 2. The compressive stress–strain curves for different volume fraction $W_f/Zr_{41.2}Ti_{13.8}Cu_{12.5}Ni_{10}Be_{22.5}$ BMGC reinforced with different tungsten fiber of (a) 750 µm; (b) 500 µm; (c) 200 µm in diameter at a strain rate about $6 \times 10^{-4}\, s^{-1}$.

45–60%, the composites exhibited high compressive strength and large plastic strain. However, once the W_f volume fraction exceeded 60%, the compressive strength and plastic strain of the $W_f/Zr_{41.2}Ti_{13.8}Cu_{12.5}Ni_{10}Be_{22.5}$ BMGC decreased.

From Fig. 2(a), it is found that the 25% (volume fraction) W_f reinforced BMGC gives 2% plastic strain, when W_f volume fraction increases to 50%, the compressive strength and plastic strain of the composites were increased to 1912 MPa and 9%, respectively. Further, when the W_f volume fraction goes to 56%, the compressive strength reaches 1936 MPa, but the plastic strain decreased to 4.8%, while 61% volume fraction $W_f/Zr_{41.2}Ti_{13.8}Cu_{12.5}Ni_{10}Be_{22.5}$BMGC only showed 0.3% plastic

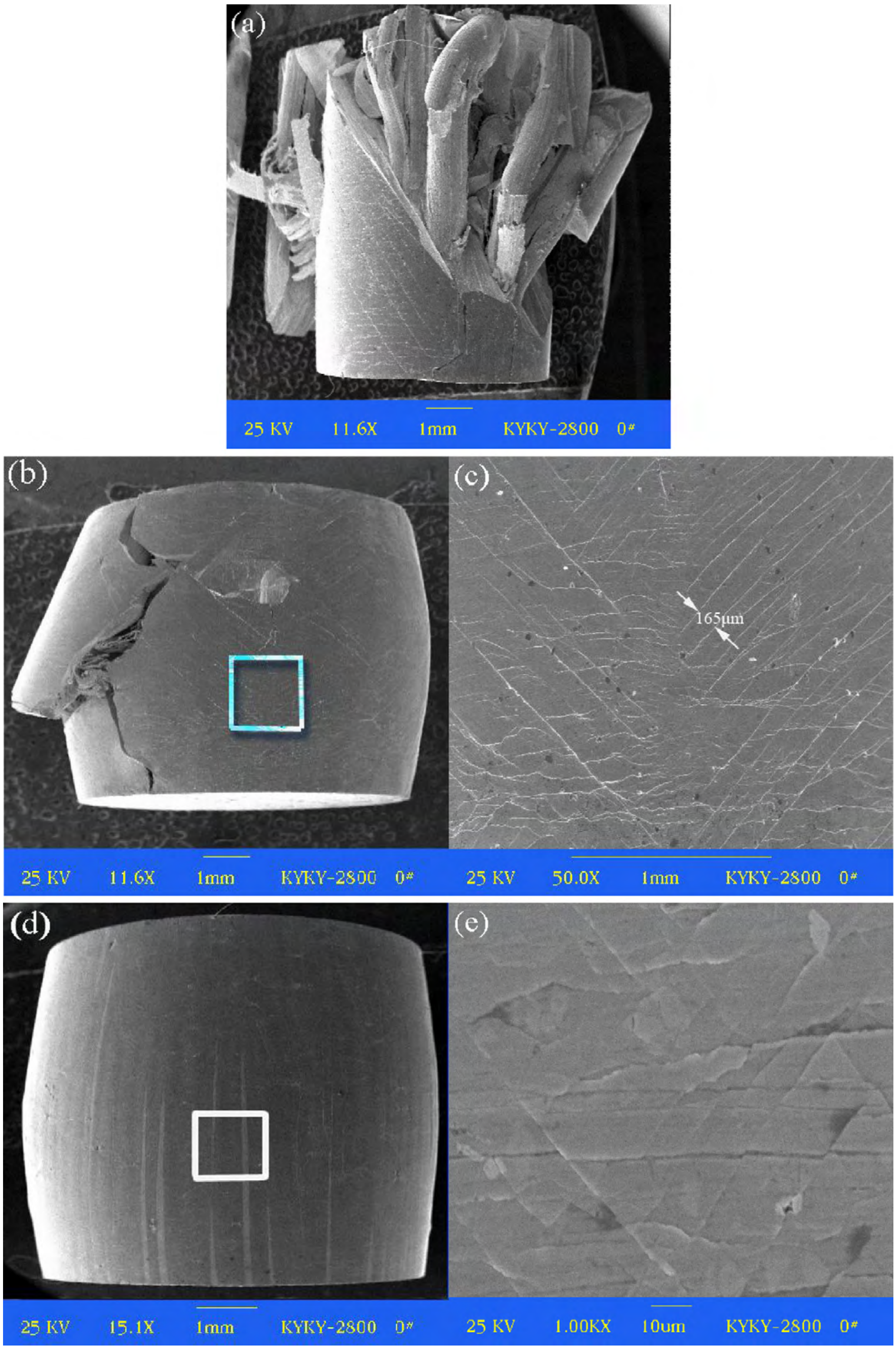

Fig. 3. Compressive fracture surface of $W_f/Zr_{41.2}Ti_{13.8}Cu_{12.5}Ni_{10}Be_{22.5}$ BMGC reinforced with 50% volume fraction tungsten fibers of (a) 750 μm; (b) 500 μm; (d) 200 μm in diameter. (c) and (e) are the local magnification of the areas labeled in (b) and (d).

strain. For the $W_f/Zr_{41.2}Ti_{13.8}Cu_{12.5}Ni_{10}Be_{22.5}$ BMGC reinforced with W_f of 500 μm in diameter, as shown in Fig. 2(b), the specimens reinforced with 30%, 40% volume fraction W_f exhibited almost no plastic strain, when the W_f volume fraction reached to 45%, the compressive strength and plastic strain increased markedly to 1875 MPa and 7.6%, increased the W_f volume fraction unceasingly to 50% and 60%, the $W_f/Zr_{41.2}Ti_{13.8}Cu_{12.5}Ni_{10}Be_{22.5}$ BMGC exhibited tremendous plastic strain of 18.4% and 17.2%, respectively. Compared to the BMGC reinforced with W_f of 500 μm in diameter, $W_f/Zr_{41.2}Ti_{13.8}Cu_{12.5}Ni_{10}Be_{22.5}$ BMGC reinforced with W_f of 200 μm in diameter had the similar trend and exhibited the highest plastic strain of 21.4% when W_f volume fraction reached 50% (Fig. 2(c)). Interestingly, $W_f/Zr_{41.2}Ti_{13.8}Cu_{12.5}Ni_{10}Be_{22.5}$ BMGC reinforced with the three kinds of W_f exhibited some work-hardening rather than perfectly plastic behavior.

Fig. 3 shows compressive fracture surface of $W_f/Zr_{41.2}Ti_{13.8}Cu_{12.5}Ni_{10}Be_{22.5}$ BMGC reinforced with 50% volume fraction tungsten fibers. Fig. 3(a) shows the fracture surface of the specimen reinforced with W_f of 750 μm in diameter, delaminating, buckling, tilting and splitting of tungsten fibers and multiple shear bands could be clearly observed. A shear band spacing of approximately 200 μm also can be identified in the matrix. Fig. 3(b) shows the compressive fracture surface morphology of $Zr_{41.2}Ti_{13.8}Cu_{12.5}Ni_{10}Be_{22.5}$ BMGC reinforced with 50% volume fraction W_f of 500 μm in diameter. It is argued that macroscopical cracks running through the sample resulted in the failure of the BMGC sample, numerous shear bands oriented at $\pm 45^{\circ}$ to the axis uniformly distributed in the matrix. Fig. 3(c) shows the magnified picture of the specific area in Fig. 3(b), and the shear band spacing of 50–100 μm were observed in the matrix. Fig. 3(d) shows the compressive surface morphology of $Zr_{41.2}Ti_{13.8}Cu_{12.5}Ni_{10}Be_{22.5}$ BMGC reinforced with 50% volume fraction tungsten fiber of 200 μm in diameter. It is observed that despite the sample had already achieved 13% plastic strain, the surface of the BMGC sample is apparently smooth and no macroscopic cracks were visible. However, if we take a closer look at the surface, many micro-cracks with a length of approximately 50 μm and shear band spacing of ~10 μm were found. Fig. 3(e) shows the specific area in Fig. 3(d) and the shear band spacing of ~10 μm is visible. Clearly, the failure mode always follows fiber longitudinal buckling.

Quasi-static compression tests on the $Zr_{41.2}Ti_{13.8}Cu_{12.5}Ni_{10}Be_{22.5}$ BMGC reinforced with W_f showed that failure mode depends upon the fiber volume fraction [15]. It is also reported that the failure mode varied with fiber type [10]. It is summarized that when the W_f volume fraction was less than 40%, fiber reinforced $Zr_{41.2}Ti_{13.8}Cu_{12.5}Ni_{10}Be_{22.5}$ BMGC samples failed mainly by localized shear banding; once the W_f volume fraction increased to 40%, the quasi-static failure mode changed from shear to fiber splitting, buckling, and localized tilting [15], and when W_f volume fraction exceeded 60%, $Zr_{41.2}Ti_{13.8}Cu_{12.5}Ni_{10}Be_{22.5}$ BMGC samples failed mainly by longitudinal splitting [10], which were in accord with our experiment results. However, when the volume fraction was between 40% and 60%, the failure mode probably related to the interface condition. In our experiment, the failure mode was also dependent on the diameter of tungsten fiber. The liquid–solid surface area of W_f (200 μm in diameter) reinforced composites was 2.5 times of that of W_f (500 μm in diameter) reinforced composites. It appears that thinner tungsten fibers produce larger surface area to prevent shear bands expanding. This has been confirmed by the shear banding spacing of the BMG composites reinforced with different tungsten fibers.

4. Conclusions

(1) $W_f/Zr_{41.2}Ti1_{3.8}Cu_{12.5}Ni_{10}Be_{22.5}$ bulk metallic glass composites were successfully prepared by an inverted melt infiltrating method.
(2) The $W_f/Zr_{41.2}Ti1_{3.8}Cu_{12.5}Ni_{10}Be_{22.5}$ bulk metallic glass composites reinforced with 50% volume fraction W_f of 200 μm in diameter exhibited high compressive strength and plastic strain of 2146 MPa, 21.4%, respectively.
(3) Thinner tungsten fibers favor to introduce more interfaces to keep shear bands from expanding, and to produce narrower shear band spacing.

Acknowledgements

This work was supported by the NSFC (Grant Nos. 50731005, 50821001 and 50944029), NBRPC (Grant Nos. 2010CB731600 and 2006CB605201), PCSIRT (Grant No. IRT0650), and DHRSS of Hebei.

References

[1] A. Inoue, Acta Mater. 48 (2000) 279–306.
[2] R.B. Dandliker, R.D. Conner, W.L. Johnson, J. Mater. Res. 13 (1998) 2796–2798.
[3] H. Choi-Yim, R.D. Conner, Scripta Mater. 45 (2001) 1039–1045.
[4] W.H. Wang, C. Dong, C.H. Shek, Mater. Sci. Eng. R 44 (2004) 45–89.
[5] Z. Bian, H. Kato, C.L. Qin, W. Zhang, A. Inoue, Acta Mater. 53 (2005) 2037–2048.
[6] H.A. Bruck, T. Christman, A.J. Rosakis, W.L. Johnson, Scripta Metall. Mater. 30 (4) (1994) 429.
[7] H.A. Bruck, A.J. Rosakis, W.L. Johnson, J. Mater. Res. 11 (2) (1996) 503.
[8] C.J. Gilbert, R.O. Ritchie, W.L. Johnson, Appl. Phys. Lett. 71 (4) (1997) 476.
[9] A.T. Alpas, J.D. Embury, Scripta Metall. 22 (2) (1988) 265.
[10] R.D. Conner, R.B. Dandliker, W.L. Johnson, Acta Mater. 46 (1998) 6089–6102.
[11] H. Choi-Yim, R. Busch, U. Kőhster, et al., Acta Mater. 47 (1999) 2455–2462.
[12] H. Choi-Yim, R. Busch, W.L. Johnson, J. Appl. Phys. 83 (1998) 7993–7997.
[13] X.F. Wu, K.Q. Qiu, H.F. Zhang, et al., Acta Metall. Sinica 39 (2003) 414–418.
[14] Y.K. Xu, J. Xu, Scripta Mater. 49 (2003) 843–848.
[15] R.D. Conner, R.B. Dandliker, V. Scruggs, W.L. Johnson, Int. J. Impact Eng. 24 (2000) 435–444.
[16] G.J. Fan, H.J. Fecht, E.J. Lavernia, Appl. Phys. Lett. 84 (2004) 487–489.
[17] W.F. Ma, H.C. Kou, C.S. Chen, J.S. Li, H. Chang, L. Zhou, H.Z. Fu, Mater. Sci. Eng. A 486 (2008) 308–312.